European Journal of Remote Sensing

ISSN: 2279-7254 (Online) Journal homepage: www.tandfonline.com/journals/tejr20

Analytical study of land surface temperature with NDVI and NDBI using Landsat 8 OLI and TIRS data in Florence and Naples city, Italy

Subhanil Guha, Himanshu Govil, Anindita Dey & Neetu Gill

To cite this article: Subhanil Guha, Himanshu Govil, Anindita Dey & Neetu Gill (2018) Analytical study of land surface temperature with NDVI and NDBI using Landsat 8 OLI and TIRS data in Florence and Naples city, Italy, European Journal of Remote Sensing, 51:1, 667-678, DOI: 10.1080/22797254.2018.1474494

To link to this article: https://doi.org/10.1080/22797254.2018.1474494

Published online: 02 Jun 2018.

EUROPEAN JOURNAL OF REMOTE SENSING, 2018
VOL. 51, NO. 1, 667–678
https://doi.org/10.1080/22797254.2018.1474494

Analytical study of land surface temperature with NDVI and NDBI using Landsat 8 OLI and TIRS data in Florence and Naples city, Italy

Subhanil Guha[a], Himanshu Govil[a], Anindita Dey[b] and Neetu Gill[c]

[a]Department of Applied Geology, National Institute of Technology Raipur, Raipur, India; [b]Department of Geography, Nazrul Balika Vidyalaya, Guma, West Bengal, India; [c]Chhattisgarh Council of Science and Technology, Raipur, India

ABSTRACT

The present study focuses on determining the relationship of estimated land surface temperature (LST) with normalized difference vegetation index (NDVI) and normalized difference built-up index (NDBI) for Florence and Naples cities in Italy using Landsat 8 data. The study also classifies different land use/land cover LU–LC) types using NDVI and NDBI threshold values, iterative self-organizing data analysis technique and maximum likelihood classifier, and analyses the relationship built by LST with the built-up area and bare land. Urban thermal field variance index was applied to determine the thermal and ecological comfort level of the city. Several urban heat islands (UHIs) were extracted as the most heated zones within the city boundaries due to increasing anthropogenic activities. The difference between the mean LST of UHI and non-UHI is 3.15°C and 3.31°C, respectively, for Florence and Naples. LST build a strong correlation with NDVI (negative) and NDBI (positive) for both the cities as a whole, especially for the non-UHIs. But, the strength of correlation becomes much weaker within the UHIs. Moreover, most of the UHIs (85.21% in Naples and 76.62% in Florence) are developed within the built-up area or bare land and are demarcated as an ecologically stressed zone.

ARTICLE HISTORY
Received 17 August 2017
Revised 26 December 2017
Accepted 6 May 2018

KEYWORDS
Land surface temperature (LST); normalized difference vegetation index (NDVI); normalized difference built-up index (NDBI); land use/land cover (LU–LC); urban thermal field variance index (UTFVI); urban heat island (UHI)

Introduction

The urban heat island (UHI) effect indicates the higher air and land surface temperature (LST) in urban areas in comparison to the surrounding rural area, generated by high levels of near-surface energy emission, solar radiation absorption of ground objects and low rates of evapotranspiration (Buyantuyev & Wu, 2010; Kleerekoper, van Esch, & Salcedo, 2012; Oke, 1982, 1997; Rizwan, Dennis, & Liu, 2008). The UHI of big cities has increased gradually since the last few decades (Akbari, Pomerantz, & Taha, 2001; Oke, 1976; Stone, 2007) with urban concentrations generating modelled and observed changes in regional temperatures (Georgescu, Moustaoui, Mahalov, & Dudhia, 2011; He, Liu, Zhuang, Zhang, & Liu, 2007; Kalnay & Cai, 2003; Li, Wang, Shen, & Song, 2004). The relationship between landscape pattern and UHI becomes globally considerable (Chen, Yao, Sun, & Chen, 2014; Coseo & Larsen, 2014; Du et al., 2016a; Du, Xiong, Wang, & Guo, 2016b; Li, Song, Cao, Meng, & Wu, 2011; Peng, Xie, Liu, & Ma, 2016). A large number of studies considered that the built-up area and bare land accelerate the effect of UHI, whereas green space and water reduce the UHI intensity (Amiri, Weng, Alimohammadi, & Alavipanah, 2009; Song, Du, Feng, & Guo, 2014). Furthermore, LST is controlled by the complex pattern of landscape composition and configuration (Asgarian, Amiri, & Sakieh, 2015; Zhou, Qian, Li, Li, & Han, 2014). Some researchers have found that natural and socio-economic factors simultaneously create certain effects on LST pattern (Buyantuyev & Wu, 2010; Jenerette et al., 2007; Kuang et al., 2015).

Landsat 5 TM and Landsat 8 OLI thermal infrared data with 120 and 100 m spatial resolutions, respectively, have been utilized for local-scale studies of UHI (Bendib, Dridi, & Kalla, 2017; Chen, Wang, & Li, 2002; Weng, 2001; Weng & Yang, 2004; Zhang et al., 2016). A variety of algorithms have been developed to retrieve LST from Landsat data, such as mono-window algorithm (Qin, Karnieli, & Berliner, 2001), single-channel algorithm (Munoz et al., 2009; Munoz & Sobrino, 2003), etc.

Urban hot spots (UHS), the special urban thermal features, experience extreme heat stress mainly developed by man-made activities within a UHI zone (Chen, Zhao, Li, & Yin, 2006; Coutts, White, Tapper, Beringer, & Livesley, 2016; Feyisa, Meilby, Jenerette, & Pauliet, 2016; Lopez, Heider, & Scheffran, 2017; Pearsall, 2017; Ren et al., 2016). So, identifying these UHS for mitigation purpose becomes an important task to maintain the ecological balance within a city.

Different scholars in different time periods attempted to draw a correlation between LST in UHIs and some land use/land cover (LU–LC) indices for different study area (Chen et al., 2006; Deilami & Kamruzzaman, 2017; Estoque, Murayama, & Myint,

CONTACT Subhanil Guha subhanilguha@gmail.com Department of Applied Geology, National Institute of Technology Raipur, Raipur, India

2017; Ma, Wu, & He, 2016; Mathew, Sreekumar, Khandelwal, Kaul, & Kumar, 2016; Mushore, Mutanga, Odindi, & Dube, 2016; Nie, Man, Li, & Huang, 2016; Tran. et al., 2017; Weng & Yang, 2004). But, LST correlates differently with LU–LC indices for a whole city or for a small UHI zone formed within the city boundary.

Italian urban areas have some special characteristics in the evolution of built-up surfaces. Italy is considered as one of the most developed European countries with artificial land cover or built-up surface. High LST is normally found within the UHI and specifically, within the UHS. There are a number of analytical research works available regarding the relationships between LST and LU–LC indices, especially in the Italian urban environment. A new linear-regression-based downscaling method of LST has been developed for Landsat 5 TM from 120 to 30 m resolution in Florence city and it has been compared with the other downscaling techniques (Bonafoni, Anniballe, Gioli, & Toscano, 2016). An interesting and innovative attempt was made in Milan, Rome, Bologna and Florence cities by using MODIS data products (1 km) to observe annual and seasonal pattern of spatial relationships between LST and built-up surfaces (Morabito et al., 2016). Another unique research work was performed to develop urban heat-related elderly risk index in 11 major Italian cities using MODIS daytime and night-time LST (Morabito et al., 2015). In Italy, inland and coastal environment can play different roles in the LST generation and in the relationship of generated LST with green areas and built-up surfaces within the urban areas.

A number of research works have been carried out to introduce some thermal comfort indices for measuring the effect of UHI intensity, i.e. temperature humidity index, physiological equivalent temperature, wet-bulb globe temperature and urban thermal field variance index (UTFVI). (Kakon, Nobuo, Kojima, & Yoko, 2010; Matzarakis, Mayer, & Iziomon, 1999; Willett & Sherwood, 2012; Zhang, 2006). Among these indices, UTFVI is the most widely used index for the ecological evaluation of urban environment due to its direct relation to LST (Alfraihat, Mulugeta, & Gala, 2016; Li et al., 2013; Liu & Zhang, 2011; Mackey, Lee, & Smith, 2012; Nichol, 2005). Determining the ecological comfort level of each and every important city is a very important task, especially for developed Italian cities.

The specific objectives of this study are: (1) to retrieve LST from Landsat 8 OLI and TIRS data and prepare spatial LST distribution maps for two Italian cities: (a) Florence – considered as an inland city and (b) Naples – considered as a coastal city; (2) to identify the UHI and non-UHI, based on the retrieved LST over the whole Florence and Naples cities; (3) to correlate LST with normalized difference vegetation index (NDVI) and normalized difference built-up index (NDBI) for the whole Florence and Naples and for the UHI and non-UHI existed within the city; (4) to build a relationship between UHI with built-up area and bare land portions of both the cities; and (5) to evaluate the thermal comfort level for both the cities using UTFVI.

Study area and data

In the present study, the spatial distribution of LST and the correlation of LST with NDVI and NDBI have been analysed in cities having Mediterranean and humid subtropical climate. Florence and Naples of Italy were selected for the research work. False colour composite (FCC) imageries of Florence and Naples city are shown in Figure 1 (Source: Unites States Geological Survey). Red colour shows the green vegetation, while blue or cyan colour presents the built-up areas. Florence is an inland city of northern Italy far away from the coastal environment, while Naples is situated on the western coast of southern Italy.

Florence is the capital city of Tuscany and metropolitan city of Italy. It is located in the Arno river basin and interlocked by a number of hills, like Careggi, Fiesole, Settignano, Arcetri, Poggio Imperiale and Bellosguardo. The latitudinal and longitudinal extension of Florence is from 43° 42′ 36″ N to 43° 50′ 24″ N and from 11° 08′ 24″ E to 11° 20′ 24″ E, respectively. Geologically, Florence is characterized by Quaternary alluvial and lacustrine deposits. The city has an elevation of 22–350 m. The soil is mainly alluvial, rich in iron oxides, clay minerals and organic matters with shallow water content. Florence is characterized by humid subtropical (Cfa) climate blended with Mediterranean (Csa) climate. Summer season is hot, while winter season is cool and moist. July and August are the hottest months, while December and January are the coldest months. The temperature of Florence often crosses the coastal temperature due to the absence of prevailing wind. Rainfall is convectional (in summer) and orographic (in winter). The mean annual temperature varies from 6°C to 25°C and average annual rainfall is about 850–900 mm [Source: World Meteorological Organisation (United Nations)]. The total area of Florence city is about 63 km^2. Florence experiences a very high density of population (3700 persons/km^2) [Source: Italian National Institute of Statistics (Italian: Istituto Nazionale di Statistica; Istat)]. Most of the residents are Italian while the majority of the immigrants come from Romania, Albania, China and the Philippines. Tourism, manufacturing, food and wine production are the dominant industries of Florence. Florence is well known for Italian fashion hub and architectural heritage.

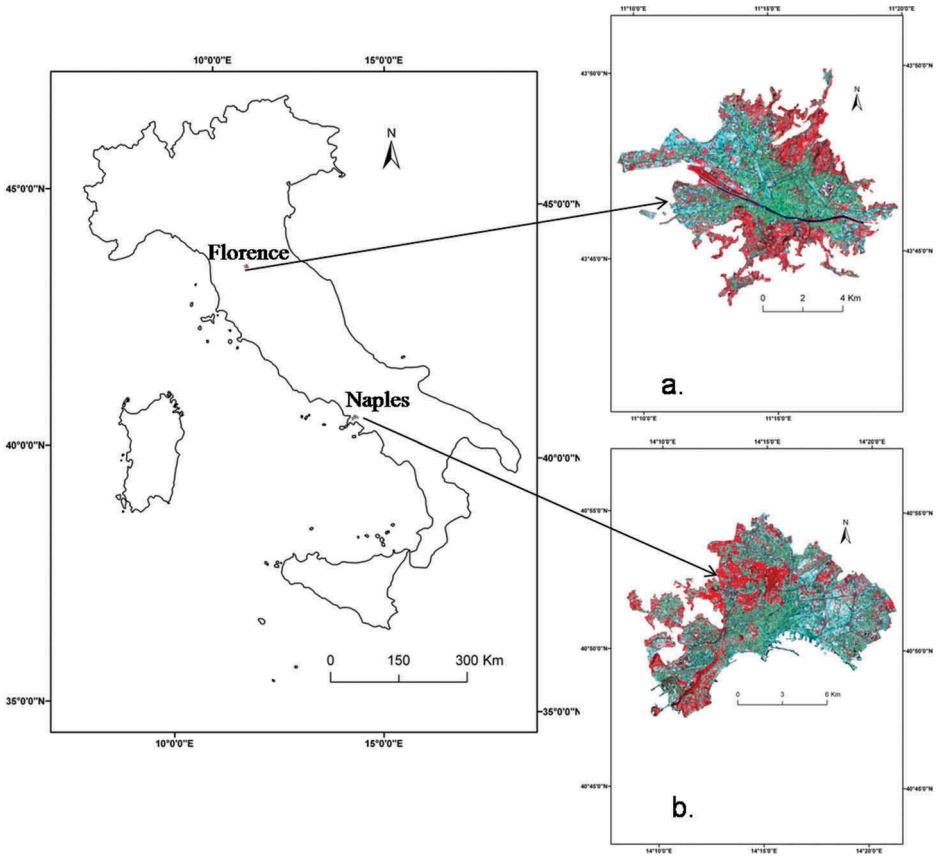

Figure 1. Location of the study area.

Naples is the capital of Campania and it is the third-largest municipality in Italy. It is located on the Gulfs of Naples and attains an elevation of 467 m from the mean sea level. It extends from 40° 47′ 24″ N to 40° 55′ 12″ N latitude and 14° 08′ 24″ E to 14° 21′ 02″ E longitude. Mount Vesuvius and Campi Fiegrei are the two nearest volcanoes. Geologically, Naples is characterized by extrusive igneous rocks, escarpment and included valleys. Volcanic soils with clay materials, iron oxides and alluvial deposits are the major soil types in Naples region. It has Mediterranean (Csa) and humid subtropical climate (Cfa) characterized by hot, dry summer and cool, wet winter. Mean annual temperature is 8–23°C and average annual rainfall is about 900–1000 mm [Source: World Meteorological Organisation (United Nations)]. Hottest months are July and August, while minimum temperature is found in December and January. Naples has an area of 107 km^2. Naples is considered as the most densely populated city in Italy with >8000 persons/km^2 [Source: Italian National Institute of Statistics (Italian: Istituto Nazionale di Statistica; Istat)]. Percentage of foreign immigrants is low compared to the cities of northern Italy. Naples is considered as the fourth-largest economy in Italy and also is listed among the UNESCO world heritage sites.

Landsat 8 OLI and TIRS data of 10 July 2016 for Florence (Figure 2(a) shows the FCC image of Florence) and of 21 July 2016 for Naples (Figure 2 (b) shows the FCC image of Naples) were used to determine the LST and to detect the UHI and UHS during the summer season. ASTER GLOBAL DEM data of 17 October 2011 for Florence (ASTGDEMV2_0N43E011) and for Naples (ASTGDEMV2_0N40E014) were used to get the information regarding elevation (Figure 2(c) and (d)). The ASTER DEM data sets (Source: Unites States Geological Survey) were georeferenced and resampled at 30 m resolution to match the Landsat data set. These elevation data were very helpful to understand the relationships between LST–NDVI and LST–NDBI.

The Landsat 8 OLI and TIRS data sets were created by the US Geological Survey and were obtained in geographically tagged image file format (GeoTIFF). The data specification of Landsat 8 OLI and TIRS sensor is shown above (Table 1). Landsat 8 TIRS data set has two bands (band 10 and band 11) with thermal characteristics. Due to the larger calibration uncertainty associated with band 11, it is recommended that users should work with band 10 data as a single spectral band and should not attempt a split-window algorithm using both bands 10 and 11. The optical bands have been used in developing NDVI and NDBI. High-resolution Google Earth image was used as the reference data for LU–LC identification. ERDAS Imagine 9.1 and ArcGIS 9.3

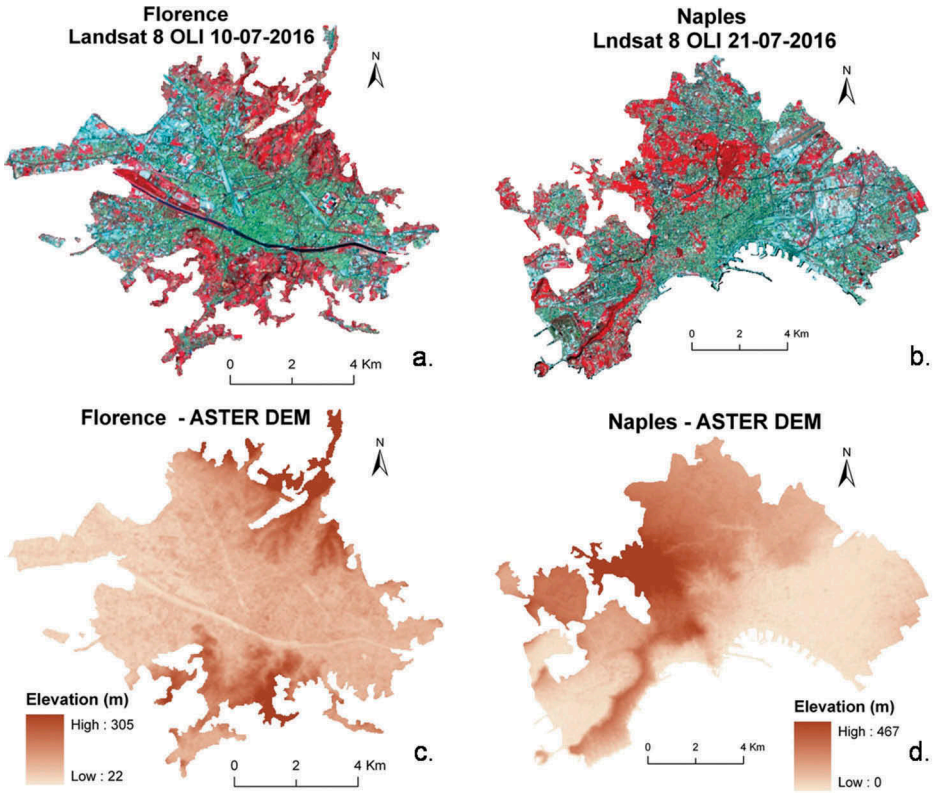

Figure 2. Satellite imageries of the study area: (a) FCC image of Landsat 8 OLI-Florence; (b) FCC image of Landsat 8 OLI- Naples; (c) ASTER DEM-Florence; (d) ASTER DEM-Naples.

Table 1. Landsat 8 OLI and TIRS data specification for Florence and Naples cities.

Place	Path/Row	Time	Date of acquisition	Sun elevation (°)	Sun azimuth (°)	Cloud cover (%)	Earth–Sun distance (AU)
Florence	192/030	09:59:05	10 July 2016	62.93	134.46	1.76	1.02
Naples	189/032	09:41:24	21 July 2016	62.87	131.08	0.74	1.02

AU: Astronomical Unit.

were used as remote sensing and GIS software to analyse the data and obtain the final output throughout the entire study.

Methodology

The overall methodology of the present study has been presented in a flowchart (Figure 3).

Image preprocessing

The satellite data acquired from the Landsat 8 sensor were subset to limit the data size. First of all, the satellite imageries were geometrically and radiometrically corrected to enhance the image quality. The thermal infrared band (band 10) for Landsat 8 TIRS image has a spatial resolution of 100 m. This thermal band was resampled using the nearest neighbour algorithm with a pixel size of 30 m to match the optical bands. To analyse the changes in temperature and LU–LC types in the study region, the NDVI and NDBI were applied for determining the correlation with derived LST.

Extraction of different LU–LC types using NDVI and NDBI

The NDVI (Purevdorj, Tateishi, Ishiyama, & Honda, 1998; Tucker, 1979) is the most common and widely used index for vegetation extraction which was applied in this study. NDBI (Zha, Gao, & Ni, 2003) was also applied in this study to detect the built-up area. These two indices can be applied to categorize different types of LU–LC (Chen et al., 2006) by the suitable threshold values. To get more accurate classification, boolean operators may be used on the spectral bands of the indices. For example, NDVI > 0.2 and NDBI < 0 may be used together to extract vegetation. Similarly, NDVI < 0 and NDBI < 0 may be used together to extract water bodies, whereas 0 < NDVI < 0.2 and NDBI > 0.1 may be used together to extract built-up area and bare land. But these threshold values may differ due to atmospheric conditions. These values may also be integrated for LU–LC classification (Chen et al., 2006). An iterative self-organizing data analysis technique classifier with the unsupervised clustering method and the maximum likelihood classification were used later to get a better result in extracting the built-up area and bare land. The values of kappa

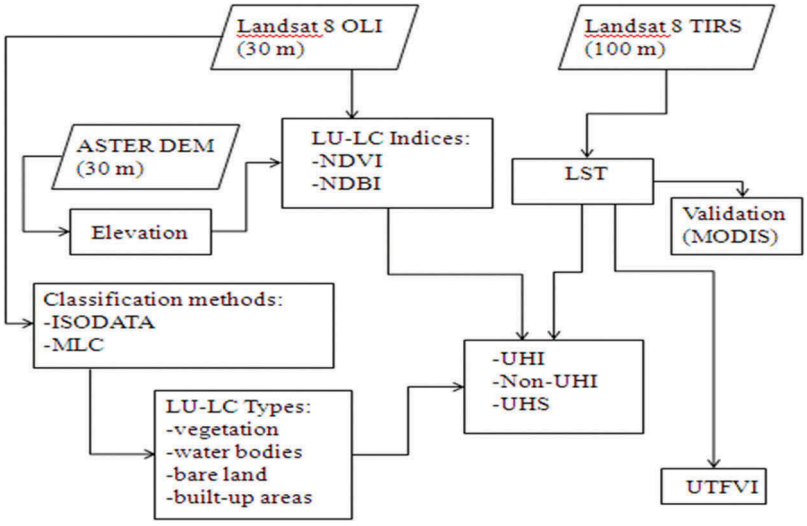

Figure 3. Flowchart of the methodology.

coefficient and overall accuracy were calculated as 0.89 and 92.36, respectively.

Retrieving LST from Landsat thermal band

LST was retrieved from band 10 of the Landsat 8 OLI and TIRS image of Florence and Naples cities using the following algorithm (Artis & Carnahan, 1982):

$$L_\lambda = 0.0003342^{*}DN + 0.1 \quad (1)$$

where L_λ is the spectral radiance in $Wm^{-2}sr^{-1}mm^{-1}$.

$$T_B = \frac{K_2}{\ln((K_1/L_\lambda)+1)} \quad (2)$$

where T_B is the brightness temperature in Kelvin (K), L_λ is the spectral radiance in $Wm^{-2}sr^{-1}mm^{-1}$; K_2 and K_1 are calibration constants. For Landsat 8 OLI, K_1 is 774.89 and K_2 is 1321.08.

The surface emissivity,ε, was estimated using the NDVI thresholds method (Sobrino, Munoz, & Paolini, 2004; Sobrino, Raissouni, & Li, 2001). The fractional vegetation,F_v, of each pixel was determined from the NDVI using the following equation (Carlson & Ripley, 1997):

$$F_v = \left(\frac{NDVI - NDV\ \mathrm{Im}\ in}{NDV\ \mathrm{Im}\ ax - NDV\ \mathrm{Im}\ in}\right)^2 \quad (3)$$

where $NDVI_{\mathrm{m}\ in}$ is the minimum NDVI value (0.2) where pixels are considered as bare soil and $NDVI_{\mathrm{m}\ ax}$ is the maximum NDVI value (0.5) where pixels are considered as healthy vegetation.

$d\varepsilon$ is the effect of the geometrical distribution of the natural surfaces and internal reflections. For heterogeneous and undulating surfaces, the value of d_ε may be 2%.

$$d\varepsilon = (1-\varepsilon_s)(1-F_v)F\varepsilon_v \quad (4)$$

where ε_v is vegetation emissivity, ε_s is soil emissivity, F_v is fractional vegetation and F is a shape factor whose mean is 0.55 (Sobrino et al., 2004).

$$\varepsilon = \varepsilon_v F_v + \varepsilon_s(1-F_v) + d\varepsilon \quad (5)$$

where ε is emissivity. From Equations (4) and (5), ε may be determined by the following equation:

$$\varepsilon = 0.004^{*}F_v + 0.986 \quad (6)$$

Finally, the LST was derived using the following equation (Weng, Lu, & Schubring, 2004):

$$LST = \frac{T_B}{1 + (\lambda\sigma T_B/(hc))\ln\varepsilon} \quad (7)$$

where λ is the effective wavelength (10.9 mm for band 10 in Landsat 8 data), σ is Boltzmann constant (1.38×10^{-23} J/K), h is Plank's constant (6.626×10^{-34} Js), c is the velocity of light in a vacuum (2.998×10^{-8} m/sec) and ε is emissivity.

Mapping UHI

UHI and non-UHI were identified by the range of LST determined by the following equations (Ma, Kuang, & Huang, 2010; Guha, Govil, & Mukherjee, 2017):

$$LST > \mu + 0.5^{*}\delta \quad (8)$$

$$0 < LST \leq \mu + 0.5^{*}\delta \quad (9)$$

where μ and δ are the mean and standard deviation of LST in the study area, respectively.

Delineating the UHS

In this study, LST maps were used in delineating the UHS over Florence and Naples to provide special emphasis for continuous monitoring. These small pockets are too hot and unfavourable for human settlement and mostly developed within the UHI.

These UHS were delineated by the following equation (Guha, Govil, & Mukherjee, 2017):

$$LST > \mu + 2 * \delta \quad (10)$$

The urban thermal field variance index (UTFVI)

A number of thermal comfort indices are available for evaluating the UHI impacts on the quality of urban life. In this study, the UTFVI has been used for the ecological evaluation of UHI zones of Florence and Naples cities in a dry summer month. UTFVI has been estimated using the following equation (Zhang, 2006):

$$\text{UTFVI} = \frac{T_s - T_{\text{mean}}}{T_{\text{mean}}} \quad (11)$$

where UTFVI= Urban Thermal Field Variance Index
T_s= LST (°C)
T_{mean}= Mean LST (°C)

Results and discussion

Spatial distribution of LST, NDVI and NDBI

Table 2 presents the descriptive statistics of LST, NDVI and NDBI values for both the cities. LST distribution was classified into appropriate ranges (Figure 4) and colour-coded to generate a thermal pattern distribution map of LST over the study area. The mean LST values are 32.84°C and 33.11°C for Florence and Naples, respectively. The threshold values for UHI generation are 33.81°C and 34.24°C for Florence and Naples, respectively. A little heterogeneity in LST was observed due to the LU–LC dynamics. The high rate of activities in manufacturing and transport sector along with power generation accelerate the mean LST. The mean NDVI values for Florence and Naples are 0.25 and 0.20, respectively. The mean NDBI value is −0.06 for both the cities. Both the cities have an almost similar range of statistical data regarding LST, NDVI and NDBI.

Validation of derived LST with respect to MODIS data

Before performing any kind of application process, a validation of derived LST is very necessary with *in situ* measurement or with another type of satellite sensor. In the present research, MODIS data were used to validate the LST values as a reference image. MODIS and any Landsat sensors do not provide quality images for a same study area in a specific acquisition date. Thus, MOD11A1 data (1 km resolution) of 11 July 2016 have been taken instead of 10 July 2016 for Florence city, and MOD11A1 data (1 km resolution) of 22 July 2016 have been taken instead of 21 July 2016 for Naples city. No precipitation or atmospheric disturbances occurred in between the acquisition date of both Landsat 8 and MOD11A1 imageries. Spatial resolution of thermal infrared band is 1 km for MOD11A1 data and 100 m for Landsat 8 data. Without performing any upscaling of Landsat 8 data or downscaling of MOD11A1 data, a strong positive correlation (0.61 for Florence city and 0.56 for Naples city) was determined between the LST values estimated from Landsat 8 data and MOD11A1 data.

Spatial distribution of UHI and non-UHI

The intensity of UHI may be defined as the difference between the average temperature of UHI and non-UHI (Table 3). In Florence, the UHI zones consistently extend from west to east along the central part of the city, while in Naples UHI zones are developed in the entire eastern portion along with the western parts (Figure 5). The threshold value of UHI is estimated at 33.81°C for Florence and 34.24°C for Naples. For UHI in both the cities, the standard deviation values of LST show more variability than non-UHI. On an average, the calculated mean LST values of UHI are 3.15°C and 3.31°C more than the calculated mean LST values of non-UHI for Florence and Naples, respectively.

Identification of UHS

UHS were more abundant in the built-up areas along the western and central parts of Florence and eastern parts of Naples due to lack of both vegetation and shadows despite the higher albedo of exposed surface (Figure 6). The UHS were identified by a threshold value of 36.72°C and 37.61°C for Florence and Naples, respectively. Parking area, roadways, power plants, metal roofs and industrial factories are most suitable places for the development of UHS. Almost all such hot spots have a very little or negligible amount of vegetation and water bodies.

Table 2. Descriptive statistics of LST, NDVI and NDBI for Florence and Naples cities.

	LST (°C)				NDVI				NDBI			
	Min	Max	Mean	SD	Min	Max	Mean	SD	Min	Max	Mean	SD
Florence	26.34	41.70	32.84	1.94	−0.17	0.61	0.25	0.12	−0.40	0.45	−0.06	0.10
Naples	22.11	41.27	33.11	2.25	−0.10	0.62	0.20	0.13	−0.38	0.30	−0.06	0.09

Min: Minimum; Max: Maximum; SD: Standard deviation.

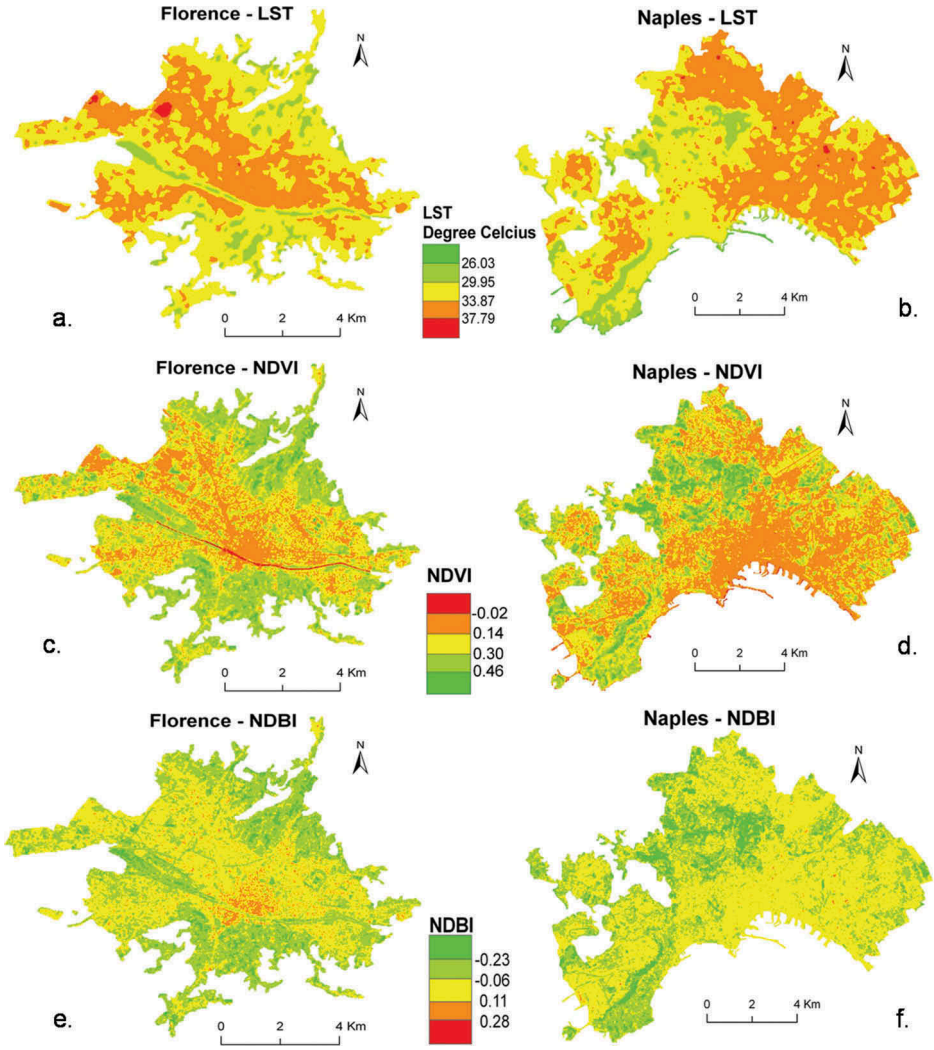

Figure 4. Spatial distribution Map of LST: (a) Florence and (b) Naples; NDVI: (c) Florence and (d) Naples; and NDBI: (e) Florence and (f) Naples.

Table 3. Variation of LST (°C) in UHI and non-UHI.

	LST(Min)		LST(Max)		LST(Mean)		LST(SD)	
Place	UHI	non-UHI	UHI	non-UHI	UHI	non-UHI	UHI	non-UHI
Florence	33.81	26.34	41.70	33.81	34.86	31.71	0.88	1.38
Naples	34.24	22.11	41.27	34.24	35.24	31.93	0.73	1.92

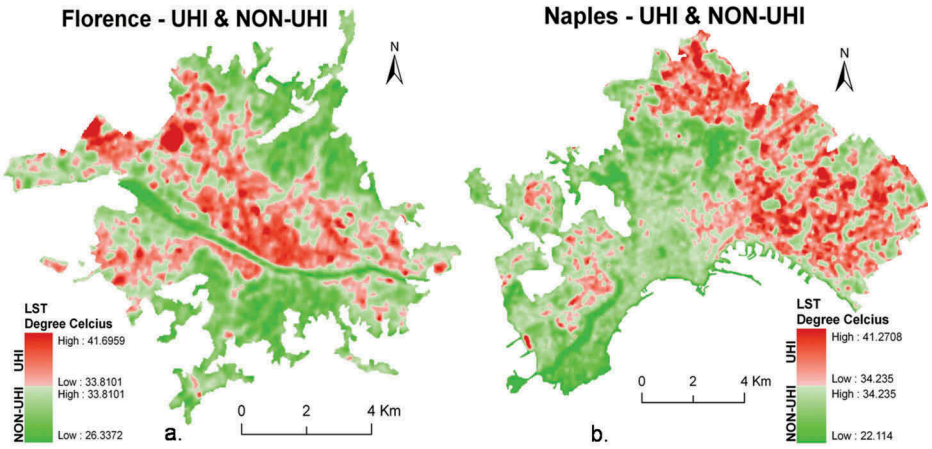

Figure 5. Spatial extents of UHI and non-UHI in Florence (a) and Naples (b).

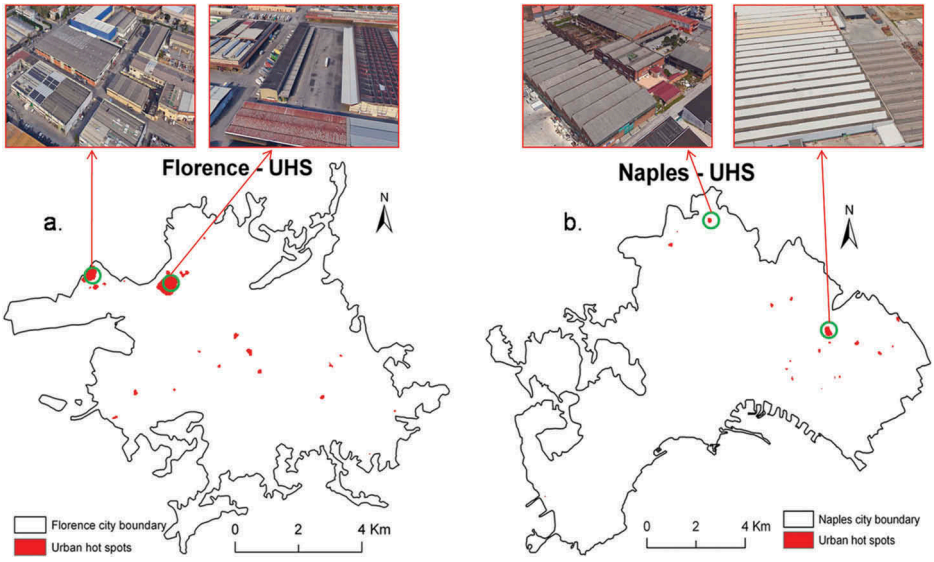

Figure 6. Location of UHS within Florence (a) and Naples (b) city boundary.

Relationship of LST–NDVI and LST–NDBI within the whole city, within the UHI and within the non-UHI

In general, LST presents a positive relationship with NDBI and an inverse relationship with NDVI. NDVI shows a strong negative correlation with LST for the whole city (−0.71 for Florence and −0.57 for Naples) and for the non-UHI (−0.53 and −0.42, respectively, for Florence and Naples). This strength becomes weaker for UHI (−0.38 for Florence and −0.19 for Naples). NDBI presents a highly positive correlation with LST for the whole city (0.71 for Florence and 0.61 for Naples) and for the non-UHI (0.61 and 0.50, respectively, for Florence and Naples). But in UHI, the value of correlation coefficient becomes much lower (0.21 for both the cities). This phenomenon is observed due to the presence of complexity in landscape composition. Thus, LST–NDVI and LST–NDBI both build stronger correlation in large natural landscapes, while it tends to be weaker in small built-up areas.

Relationship of LST with LU–LC types

It is very interesting fact that LST distribution is very closely related to the distribution of NDVI and NDBI. Generally, LST is negatively related to NDVI and positively related to NDBI. But, this relationship may be varied due to spatial resolution, latitudinal extension or seasonal variation. Florence and Naples are the two major cities of Italy; one is located in the inland northern part while other lies in the coastal southern part. Both the cities support the general relationship of LST with NDVI and NDBI. NDVI and NDBI are the two LU–LC indices those are highly dependent on the LU–LC types in any region. Normally, high NDVI values indicate the presence of green vegetation and high NDBI values indicate the presence of built-up area and bare land. Basically, LST increases with the increase in built-up area and bare land whereas it decreases with the increase in forest, cropland, wetland and water bodies.

Figure 7 describes the built-up area and bare land of Florence and Naples cities with the help of the separate bands of Landsat data, LU–LC indices and Google Earth image. Built-up area and bare land together cover 25.18 km^2 area of Florence, i.e. 39.91% of the total city area of Florence, and cover 61.88 km^2 area of Naples, i.e. 57.95% of the total city area of Naples. Thus, Naples is considered as more urbanized city than Florence. Vegetation, river, water bodies, wetlands and croplands have been described as the other lands.

Figure 8 presents a very important relationship of UHI with the built-up area and bare land. In Florence, 35.93% area is under UHI while in Naples it is almost equal (35.78%). But, the percentage of UHI in the total built-up area and bare land is significantly high in Naples (85.21%) compared to Florence (76.62%). In Florence, 23.38% of UHI zones are developed outside the built-up area and bare land. Thus, the relationship of UHI with the built-up area and bare land is stronger in Naples.

Table 4 reflects the correlation between elevation with LST and LU–LC indices. There is no significant difference found in the relationships between elevation and NDVI (positive correlation) or elevation and NDBI (negative correlation) for Florence and Naples. But, Florence reflects a stronger negative correlation between elevation and LST.

Ecological evaluation of Florence and Naples using UTFVI

The UTFVI values were divided into six categories (Zhang, 2006) according to six different ecological evaluation indices (Table 5).

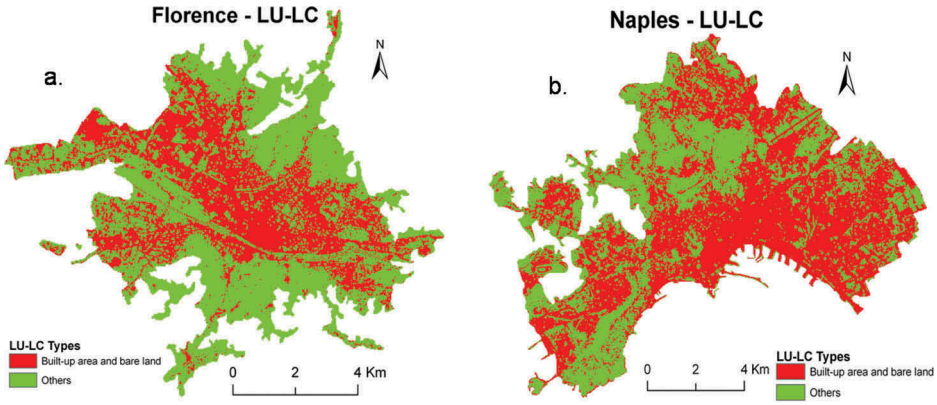

Figure 7. Extraction of built-up area and bare land within Florence (a) and Naples (b) city boundary.

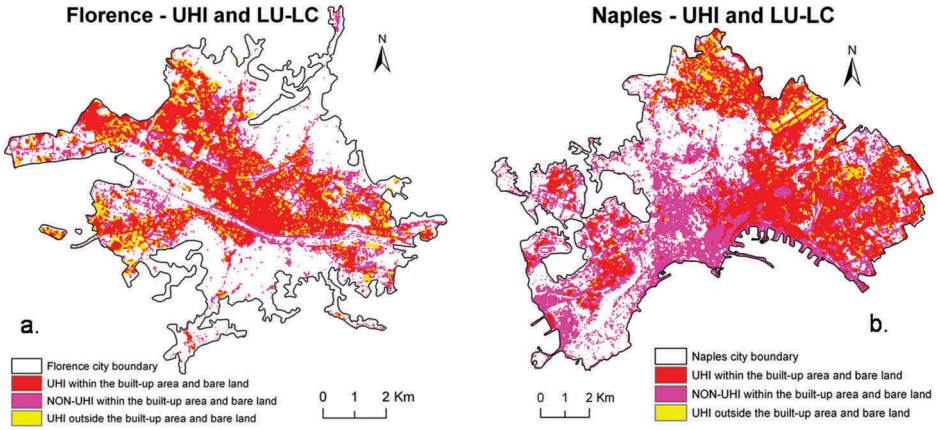

Figure 8. Relationship of UHI and non-UHI with LU–LC types within Florence (a) and Naples (b) city boundary.

Table 4. Correlation coefficient values of elevation with LST, NDVI and NDBI.

	Elevation-LST	Elevation-NDVI	Elevation-NDBI
Florence	−0.47	0.36	−0.28
Naples	−0.31	0.36	−0.32

Table 5. The threshold of ecological evaluation index.

			Percentage of area (%)	
UTFVI	UHI phenomenon	Ecological evaluation index	Florence	Naples
<0.000	None	Excellent	46.50	43.10
0.000–0.005	Weak	Good	2.60	2.94
0.005–0.010	Middle	Normal	2.75	3.13
0.010–0.015	Strong	Bad	2.79	3.10
0.015–0.020	Stronger	Worse	3.08	3.23
>0.020	Strongest	Worst	42.28	44.5

It is clear from the Figure 9 that both the cities have shared almost equal percentage of land for two extreme categories of ecological evaluation: the excellent category (UTFVI < 0) and the worst category (UTFVI > 0.020). The areas enjoy excellent thermal conditions (i.e. UTFVI < 0), where vegetation, water bodies and wetlands are abundant. Mainly, the north-eastern and the south-western portions of Florence and the central and the south-western parts of Naples (grey-coloured portions) experience such thermal condition. But, the worst category (i.e. UTFVI > 0.020) of the ecological evaluation index also exists in a large portion of both the cities (Red-coloured portions). The strip extends from north-west to south-east section of Florence and the entire eastern part of Naples, which fall under the worst category. Here, most of the lands are impervious in nature (either bare land with exposed rock surface or built-up areas). The good and the normal thermal conditions (i.e. 0 < UTFVI < 0.010) are found in some small patches surrounding the areas under excellent condition, while the bad and the worse conditions (i.e. 0.010 < UTFVI < 0.020) exist around the areas of built-up class.

Conclusion

In this article, Landsat 8 OLI and TIRS data were used to investigate the UHI intensity effect in Florence and Naples cities in Italy and to interpret the dynamic relationship between LST with NDVI and NDBI. UHI zones were identified through LST which were distributed along the central region extends from north-west to south-east portions of Florence while it develops throughout the eastern part of Naples. Bare land and built-up area are mostly responsible for LST generation. The

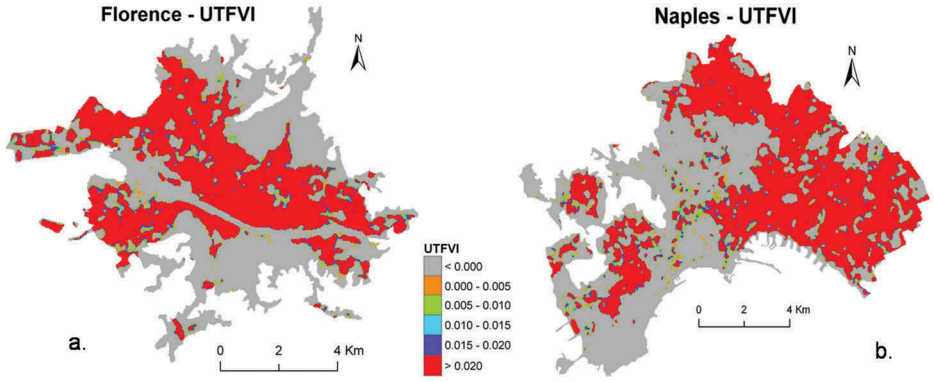

Figure 9. Ecological evaluation index of Florence (a) and Naples (b) according to UTFVI.

presence of vegetation and water bodies reduces the LST level. Some UHS were also delineated within the UHI zones which are characterized by high concentrated LST.

Furthermore, the relationships between LST–NDVI and LST–NDBI were interpreted quantitatively by linear regression analysis at the pixel level. For whole Florence and Naples cities, LST shows strong negative correlation (−0.71and −0.57) with NDVI; and strong positive correlation (0.71 and 0.61) with NDBI. The relationships become weaker for UHI. It may be due to the presence of more heterogeneous landscapes within the built-up area.

In addition, spatio-temporal dynamics of the ecological evaluation index of Florence and Naples were computed by UTFVI. Almost equal percentage of land is in excellent condition and worst condition simultaneously. It indicates that non-UHI zones (green areas and water bodies) remain almost unchanged or very little changed. Only the UHI zones are under severe heat stress. With consistent urban development, the UHI zones may worsen the eco-environmental quality and fall under worst ecological index.

In future, many additional research works may be included. First, LST may be retrieved using another method or different spatial resolution. Second, the *in situ* LST data may be measured with the same overpass of satellites for the calibration and validation of LST estimation. Third, apart from linear regression, several new statistical methods can be applied to estimate the correlation between LST and different LU–LC indices. Finally, ecological evaluation of UHI zones may be analysed with the inclusion of more biophysical parameters.

Acknowledgement

The authors are indebted to USGS server (http://earthexplorer.usgs.gov/).

Disclosure statement

No potential conflict of interest was reported by the authors.

References

Akbari, H., Pomerantz, M., & Taha, H. (2001). Cool surfaces and shade trees to reduce energy use and improve air quality in urban areas. *Solar Energy*, *70*(3), 295–310.

Alfraihat, R., Mulugeta, G., & Gala, T.S. (2016). Ecological evaluation of urban heat island in Chicago City, USA. *Journal of Atmospheric Pollution*, *4*(1), 23–29.

Amiri, R., Weng, Q., Alimohammadi, A., & Alavipanah, S. K. (2009). Spatial-temporal dynamics of land surface temperature in relation to fractional vegetation cover and land use/cover in the Tabriz urban area, Iran. *Remote Sensing of Environment*, *113*, 2606–2617.

Artis, D.A., & Carnahan, W.H. (1982). Survey of emissivity variability in thermography of urban areas. *Remote Sensing of Environment*, *12*(4), 313–329.

Asgarian, A., Amiri, B.J., & Sakieh, Y. (2015). Assessing the effect of green cover spatial patterns on urban land surface temperature using landscape metrics approach. *Urban Ecosystems*, *18*, 209–222.

Bendib, A., Dridi, H., & Kalla, M.I. (2017). Contribution of Landsat 8 data for the estimation of land surface temperature in Batna city, Eastern Algeria. *Geocarto International*, *32*(5), 503–513.

Bonafoni, S., Anniballe, R., Gioli, B., & Toscano, P. (2016). Downscaling Landsat land surface temperature over the urban area of Florence. *European Journal of Remote Sensing*, *49*(1), 553–569.

Buyantuyev, A., & Wu, J. (2010). Urban heat islands and landscape heterogeneity: Linking spatiotemporal variations in surface temperatures to land-cover and socioeconomic patterns. *Landscape Ecology*, *25*, 17–33.

Carlson, T.N., & Ripley, D.A. (1997). On the relation between NDVI, fractional vegetation cover, and leaf area index. *Remote Sensing of Environment*, *62*, 241–252.

Chen, A., Yao, X.A., Sun, R., & Chen, L. (2014). Effect of urban green patterns on surface urban cool islands and its seasonal variations. *Urban Forestry & Urban Greening*, *13*, 646–654.

Chen, X.C., Zhao, H.M., Li, P.X., & Yin, Z.Y. (2006). Remote sensing image-based analysis of the relationship between urban heat island and land use/cover changes. *Remote Sensing of Environment*, *104*(2), 133–146.

Chen, Y., Wang, J., & Li, X. (2002). A study on urban thermal field in summer based on satellite remote sensing. *Remote Sensing for Land Management and Planning*, *4*, 55–59.

Coseo, P., & Larsen, L. (2014). How factors of land use/land cover, building configuration, and adjacent heat sources and sinks explain urban heat islands in Chicago. *Landscape and Urban Planning*, *125*, 117–129.

Coutts, A.M., White, E.C., Tapper, N.J., Beringer, J., & Livesley, S.J. (2016). Temperature and human thermal comfort effects of street trees across three contrasting street canyon environments. *Theoretical and Applied Climatology*, *124*(55), 55–68.

Deilami, K., & Kamruzzaman, M. (2017). Modelling the urban heat island effect of smart growth policy scenarios in Brisbane. *Land Use Policy*, *64*, 38–55.

Du, H., Wang, D., Wang, Y., Zhao, X., Qin, F., Jiang, H., & Cai, Y. (2016a). Influences of land cover types, meteorological conditions, anthropogenic heat and urban area on surface urban heat island in the Yangtze River Delta urban agglomeration. *Science of the Total Environment*, *571*, 461–470.

Du, S., Xiong, Z., Wang, Y., & Guo, L. (2016b). Quantifying the multilevel effects of landscape composition and configuration on land surface temperature. *Remote Sensing of Environment*, *178*, 84–92.

Estoque, R.C., Murayama, Y., & Myint, S.W. (2017). Effects of landscape composition and pattern on land surface temperature: An urban heat island study in the megacities of southeast Asia. *Science of the Total Environment*, *577*, 349–359.

Feyisa, G.L., Meilby, H., Jenerette, G.D., & Pauliet, S. (2016). Locally optimized separability enhancement indices for urban land cover mapping: Exploring thermal environmental consequences of rapid urbanization in Addis Ababa, Ethiopia. *Remote Sensing of Environment*, *175*, 14–31.

Georgescu, M., Moustaoui, M., Mahalov, A., & Dudhia, J. (2011). An alternative explanation of the semiarid urban area "oasis effect". *Journal of Geophysical Research*, *116*, D24113.

Guha, S., Govil, H., & Mukherjee, S. (2017). Dynamic analysis and ecological evaluation of urban heat islands in raipur city, india. Journal of Applied Remote Sensing, *11*(3), 36020. http://dx.doi: 10.1117/1.JRS.11.036020.

He, J.F., Liu, J.Y., Zhuang, D.F., Zhang, W., & Liu, M.L. (2007). Assessing the effect of land use/land cover change on the change of urban heat island intensity. *Theoretical and Applied Climatology*, *90*, 217–226.

Jenerette, G.D., Harlan, S.L., Brazel, A., Jones, N., Larsen, L., & Stefanov, W.L. (2007). Regional relationships between surface temperature, vegetation, and human settlement in a rapidly urbanizing ecosystem. *Landscape Ecology*, *22*, 353–365.

Kakon, A.N., Nobuo, M., Kojima, S., & Yoko, T. (2010). Assessment of thermal comfort in respect to building height in a high-density city in the tropics. *American Journal of Engineering and Applied Sciences*, *3*(3), 545–551.

Kalnay, E., & Cai, M. (2003). Impact of urbanization and land-use change on climate. *Nature*, *423*, 528–553.

Kleerekoper, L., van Esch, M., & Salcedo, T.B. (2012). How to make a city climate-proof, addressing the urban heat island effect. *Resource Conservation Recycling*, *64*, 30–38.

Kuang, W., Liu, Y., Dou, Y., Chi, W., Chen, G., Gao, C., … Zhang, R. (2015). What are hot and what are not in an urban landscape: Quantifying and explaining the land surface temperature pattern in Beijing, China. *Landscape Ecology*, *30*, 357–373.

Li, J., Song, C., Cao, L., Meng, X., & Wu, J. (2011). Impacts of landscape structure on surface urban heat islands: A case study of Shanghai, China. *Remote Sensing of Environment*, *115*, 3249–3263.

Li, J., Wang, Y., Shen, X., & Song, Y. (2004). Landscape pattern analysis along an urban–rural gradient in the Shanghai metropolitan region. *Acta Ecologica Sinica*, *24*, 1973–1980.

Li, Z.L., Ning, H.W., Shi, W., Sobrino, J.A., Wan, Z.B., Tang, H., & Yan, G. (2013). Land surface emissivity retrieval from satellite data. *International Journal of Remote Sensing*, *34*(9–10), 3084–3127.

Liu, L., & Zhang, Y. (2011). Urban heat island analysis using the Landsat TM data and ASTER data: A case study in Hong Kong. *Remote Sensing*, *3*, 1535–1552.

Lopez, J.M.R., Heider, K., & Scheffran, J. (2017). Frontiers of urbanization: Identifying and explaining urbanization hot spots in the south of Mexico City using human and remote sensing. *Applied Geography*, *79*, 1–10.

Ma, Q., Wu, J., & He, C. (2016). A hierarchical analysis of the relationship between urban impervious surfaces and land surface temperatures: Spatial scale dependence, temporal variations, and bioclimatic modulation. *Landscape Ecology*, *31*, 1139–1153.

Ma, Y., Kuang, Y., & Huang, N. (2010). Coupling urbanization analyses for studying urban thermal environment and its interplay with biophysical parameters based on TM/ETM+ imagery. *International Journal of Applied Earth Observation and Geoinformation*, *12*(2), 110–118.

Mackey, C.W., Lee, X., & Smith, R.B. (2012). Remotely sensing the cooling effects of city scale efforts to reduce urban heat island. *Building and Environment*, *49*, 348–358.

Mathew, A., Sreekumar, S., Khandelwal, S., Kaul, N., & Kumar, R. (2016). Prediction of surface temperatures for the assessment of urban heat island effect over Ahmedabad city using linear time series model. *Energy and Buildings*, *128*, 605–616.

Matzarakis, A., Mayer, H., & Iziomon, M.G. (1999). Applications of a universal thermal index: Physiological equivalent temperature. *International Journal of Biometeorology*, *43*(2), 76–84.

Morabito, M., Crisci, A., Gioli, B., Gualtieri, G., Toscano, P., Di Stefano, V., … Dalal, K. (2015). Urban-hazard risk analysis: Mapping of heat-related risks in the elderly in major Italian cities. *PLoS One*, *10*(5), e0127277.

Morabito, M., Crisci, A., Messeri, A., Orlandini, S., Raschi, A., Maracchi, G., & Munafò, M. (2016). The impact of built-up surfaces on land surface temperatures in Italian urban areas. *Science of the Total Environment*, *551*, 317–326.

Munoz, J.C., Cristóba, J., Sobrino, J.A., Soria, G., Ninyerola, M., & Pons, X. (2009). Revision of the single-channel algorithm for land surface temperature retrieval from Landsat thermal-infrared data. *Photogrammetric Engineering & Remote Sensing*, *47*(1), 339–349.

Munoz, J.C., & Sobrino, J.A. (2003). A generalized single channel method for retrieving land surface temperature from remote sensing data. *Journal of Geophysical Research*, *108*. doi:10.1029/2003JD003480

Mushore, T.D., Mutanga, O., Odindi, J., & Dube, T. (2016). Assessing the potential of integrated Landsat 8 thermal bands, with the traditional reflective bands and derived vegetation indices in classifying urban landscapes. *Geocarto International*, 1–14. doi:10.1080/10106049.2016.1188168

Nichol, J.E. (2005). Remote sensing of urban heat islands by day and night. *Photogrammetric Engineering & Remote Sensing*, *19*, 1639–1649.

Nie, Q., Man, W., Li, Z., & Huang, Y. (2016). Spatiotemporal impact of urban impervious surface on land surface temperature in Shanghai, China. *Canadian Journal of Remote Sensing*, *42*(6), 680–689.

Oke, T.R. (1976). The distinction between canopy and boundary layer heat islands. *Atmosphere*, *14*, 268–277.

Oke, T.R. (1982). The energetic basis of the urban heat island. *Quarterly Journal of the Royal Meteorological Society*, *108*, 1–24.

Oke, T.R. (1997). *Urban climates and global change*. In A. Perry & R. Thompson (Eds.), *Applied climatology: Principles and practices* (pp. 273–287). London: Routledge.

Pearsall, H. (2017). Staying cool in the compact city: Vacant land and urban heating in Philadelphia, Pennsylvania. *Applied Geography*, *79*, 84–92.

Peng, J., Xie, P., Liu, Y., & Ma, J. (2016). Urban thermal environment dynamics and associated landscape pattern factors: A case study in the Beijing metropolitan region. *Remote Sensing of Environment*, *173*, 145–155.

Purevdorj, T.S., Tateishi, R., Ishiyama, T., & Honda, Y. (1998). Relationships between percent vegetation cover and vegetation indices. *International Journal of Remote Sensing*, *19*(18), 3519–3535.

Qin, Z., Karnieli, A., & Berliner, P. (2001). A mono-window algorithm for retrieving land surface temperature from Landsat TM data and its application to the Israel–Egypt border region. *International Journal of Remote Sensing*, *22*(18), 3719–3746.

Ren, Y., Deng, L.Y., Zuo, S.D., Song, X.D., Liao, Y.L., Xu, X.D., … Li, Z.W. (2016). Quantifying the influences of various ecological factors on land surface temperature of urban forests. *Environmental Pollution*, *216*, 519–529.

Rizwan, A.M., Dennis, L.Y.C., & Liu, C. (2008). A review on the generation, determination and mitigation of urban heat island. *Journal of Environmental Sciences*, *20*, 120–128.

Sobrino, J.A., Munoz, J.C., & Paolini, L. (2004). Land surface temperature retrieval from Landsat TM5. *Remote Sensing of the Environment*, *9*, 434–440.

Sobrino, J.A., Raissouni, N., & Li, Z.L. (2001). A comparative study of land surface emissivity retrieval from NOAA data. *Remote Sensing of the Environment*, *75*(2), 256–266.

Song, J., Du, S., Feng, X., & Guo, L. (2014). The relationships between landscape compositions and land surface temperature: Quantifying their resolution sensitivity with spatial regression models. *Landscape and Urban Planning*, *123*, 145–157.

Stone, B., Jr. (2007). Urban sprawl and air quality in large US cities. *Journal of Environmental Management*, *86*, 688–698.

Tran., D.X., Pla, F., Carmona, P.L., Myint, S.W., Caetano, M., & Kieua, P.V. (2017). Characterizing the relationship between land use land cover change and land surface temperature. *ISPRS Journal of Photogrammetry and Remote Sensing*, *124*, 119–132.

Tucker, C.J. (1979). Red and photographic infrared linear combinations for monitoring vegetation. *Remote Sensing of Environment*, *8*, 127–150.

Weng, Q. (2001). A remote sensing-GIS evaluation of urban expansion and its impact on surface temperature in Zhujiang Delta, China. *International Journal of Remote Sensing*, *22*(10), 1999–2014.

Weng, Q., Lu, D., & Schubring, J. (2004). Estimation of land surface temperature-vegetation abundance relationship for urban heat island studies. *Remote Sensing of Environment*, *89*(4), 467–483.

Weng, Q., & Yang, S. (2004). Managing the adverse thermal effects of urban development in a densely populated Chinese city. *Journal of Environmental Management*, *70*(2), 145–156.

Willett, K.M., & Sherwood, S. (2012). Exceedance of heat index thresholds for 15 regions under a warming climate using the wet-bulb globe temperature. *International Journal of Climatology*, *32*(2), 161–177.

Zha, Y., Gao, J., & Ni, S. (2003). Use of normalized difference built-up index in automatically mapping urban areas from TM imagery. *International Journal of Remote Sensing*, *24*(3), 583–594.

Zhang, Y. (2006). Land surface temperature retrieval from CBERS-02 IRMSS thermal infrared data and its applications in quantitative analysis of urban heat island effect. *Journal of Remote Sensing*, *10*, 789–797.

Zhang, Z., He, G., Wang, M., Long, T., Wang, G., Zhang, X., & Jiao, W. (2016). Towards an operational method for land surface temperature retrieval from Landsat 8 data. *Remote Sensing Letters*, *7*(3), 279–288.

Zhou, W., Qian, Y., Li, X., Li, W., & Han, L. (2014). Relationships between land cover and the surface urban heat island: Seasonal variability and effects of spatial and thematic resolution of land cover data on predicting land surface temperatures. *Landscape Ecology*, *29*, 153–167.